Environmental Science Processes & Impacts

Changes in riparian hydrology and biogeochemistry following storm events at a restored agricultural stream

Journal:	*Environmental Science: Processes & Impacts*
Manuscript ID	EM-ART-11-2018-000546.R1
Article Type:	Paper
Date Submitted by the Author:	13-Feb-2019
Complete List of Authors:	Welsh, Molly; SUNY College of Environmental Science and Forestry, Environmental Science vidon, philippe; SUNY College of Environmental Science and Forestry, Forest and Natural Resources Management McMillan, Sara; Purdue University, Agricultural and Biological Engineering

Changes in riparian hydrology and biogeochemistry following storm events at a restored agricultural stream

Molly K. Welsh, *[a] Philippe G. Vidon,[b] Sara K. McMillan[c]

[a]Division of Environmental Science, The State University of New York College of Environmental Science and Forestry, Syracuse, USA. E-mail: mkwelsh@syr.edu

[b]Department of Forest and Natural Resources Management, The State University of New York College of Environmental Science and Forestry, Syracuse, USA.

[c]Department of Agricultural and Biological Engineering, Purdue University, West Lafayette, USA.

Abstract

Quantifying changes in riparian biogeochemistry following rainfall events is critical for watershed management. Following storms, changes in riparian hydrology can lead to high rates of nutrient processing and export and greenhouse gas (GHG) release. We assessed shifts in hydrology and biogeochemistry 24 and 72 hours post-rainfall following storms of three different magnitudes in an agricultural riparian zone influenced by stream restoration in the Piedmont region of North Carolina, USA. Post-storm changes in water table height, soil moisture, groundwater flow, and lateral hydraulic gradient were related

to biogeochemical processing. Though near-field nitrate (NO_3^-) concentrations were elevated (median: 13 mg nitrogen (N) L^{-1} across storms), substantial riparian NO_3^- removal occurred (89-96%). High N removal throughout the study occurred concurrently with release of dissolved solutes (e.g., soluble reactive phosphorus [SRP]) and fluxes of gases (carbon dioxide [CO_2], nitrous oxide [N_2O], and methane [CH_4]), based on storm timing, magnitude, and intensity. A high intensity, short duration storm of low magnitude lead to release of CO_2 across the riparian zone and low SRP removal. A storm of intermediate duration/magnitude towards the beginning of the summer lead to mobilization of near-field NO_3^- and release of N_2O in the upper riparian zone and SRP in the lower riparian zone. Finally, a larger storm of longer duration lead to pronounced near-stream release of CH_4. Therefore, it is important to expand research of biogeochemical response to different types of storm events in restored riparian zones to better balance water quality goals with potential greenhouse gas emissions.

Environmental Significance Statement

Changes in the frequency and magnitude of precipitation events can have unforeseen impacts on pollutant transport, retention, and release. Shifts in riparian water table height, hydraulic gradient, groundwater flux, and soil moisture following storms were associated with nutrient processing and greenhouse gas release. An evaluation of riparian hydrology, water quality, and greenhouse gas dynamics following storm events of three different magnitudes is presented to illustrate differences in biogeochemical response. Though high soil moisture may promote nitrogen removal via denitrification,

which improves water quality, concomitant release of other contaminants, including soil-bound phosphorus, nitrous oxide, and methane can occur following storms. Storm timing, duration, magnitude, and intensity and antecedent conditions are associated with removal and release of water and air quality components of concern.

Introduction

Use of nitrogen (N) and phosphorus (P)-based fertilizers in agricultural systems has had deleterious impacts on aquatic ecosystems, resulting in nuisance algal blooms and low dissolved oxygen in receiving waters.[1,2] Efforts to reduce agricultural loadings of N and P have resulted in the adoption of riparian zones as a management tool for water quality improvement.[3,4] Though riparian zones have proven to be effective buffers for dissolved N and particulate P removal, release of constituents of concern, such as greenhouse gases (GHGs) or soluble reactive phosphorus (SRP) has been documented, particularly following shifts in water table height.[5-7] These rapid rises in water table height frequently occur following storm events, making storm and post-storm conditions potential "hot moments" of nutrient processing or transport (e.g., times when transport or process rates are enhanced).[8] Rising water tables and altered flowpaths following storms can also activate biogeochemical "hot spots" on the landscape as conditions that lead to processing are enhanced in areas with configurations conducive to microbial processing.[9]

However, biogeochemical responses to storms can vary depending on site hydrologic dynamics. Following storms, reduction in N removal efficiency in agricultural riparian zones has been documented following a rise in water tables[10] and has been correlated to frequency of high intensity precipitation events.[11] However, other studies

have shown that elevated water tables and intermittent flooding can promote denitrification, increasing N removal capacity of riparian zones.[12-14] Though riparian buffers may effectively trap sediment, and associated bound P, from overland flow, significant export of total phosphorus (TP) and SRP from restored wetlands has been documented following storm events,[15,16] and storm flow (both overland and subsurface) may account for the majority of SRP export in agricultural riparian zones.[9]

Greenhouse gas (carbon dioxide [CO_2], nitrous oxide [N_2O], and methane [CH_4]) production may be stimulated by an influx of water following precipitation;[17] GHG emissions increase following strong riparian rewetting events[18,19] and CO_2 often dominates post-storm riparian GHG fluxes in water-limited environments.[20-22] In saturated (often hydric) riparian soils, enhanced N_2O and CH_4 release may occur as high water tables may enhance nitrous oxide (N_2O) and methane (CH_4) generation but inhibit carbon dioxide (CO_2) production,[23-25] and research has confirmed antecedent conditions (dry or wet) influence biogeochemical response.[26,27] For example, Jacinthe *et al.* (2012) measured large N_2O fluxes in riparian zones following short duration flooding events and concluded that flood magnitude was more important than riparian vegetation type or successional stage in dictating N_2O flux.[28]

Compounding adverse impacts of nutrient loading and precipitation-induced changes in biogeochemistry is stream restoration. Stream restoration involves substantial modification of the stream channel and associated floodplain, which may influence environmental factors that impact biogeochemical processes, such as soil structure, organic carbon composition and quality, moisture, and hydrologic connectivity.[29-31] While the number of stream restoration projects across the nation is continuing to

increase, few studies are investigating the impacts of hydrologic shifts following precipitation events on riparian zone solute export and GHG release concurrently. In an evaluation of riparian biogeochemistry 20 years post-restoration, Vidon et al. (2014) assert that the fate and transport of N, P, and GHGs may depend on hot moments, rather than gradual seasonal changes.[18] However, when assessing biogeochemistry of restored riparian zones, post-storm sampling frequently does not occur as part of a monitoring protocol; there is a lack of current monitoring initiatives that analyze water and air chemistry concurrently, despite continued emphasis on the importance of post-restoration monitoring from the scientific community.[32-36] Therefore, to gain a comprehensive understanding of dynamics of contaminant export versus retention, it is important to target potential "hot moments" of removal or release for sampling following storms and to study water and air constituents in tandem, to evaluate potential water versus air contaminant tradeoffs.

In light of the variability in biogeochemical response following storm events and need for studies to assess different types of contaminants concurrently, we developed the following questions to guide our investigation: 1) How do antecedent conditions and storm characteristics (magnitude, intensity, and duration) impact post-storm hydrology (soil moisture, water table height, hydraulic gradient, groundwater fluxes) in the context of a restored riparian zone? 2) How do these hydrologic changes, coupled to antecedent conditions and storm characteristics, impact nitrogen and phosphorus dynamics (flushing, mobilization, export and retention), and GHG emission and consumption (source/sink behavior)? 3) How do biogeochemical shifts in this study provide insight into oxidation-

reduction (redox) processes in the context of water quality versus air quality goals and how may this insight be coupled to previous findings to guide future research?

Methods

Site Characteristics

The study site, Cook's Creek, is located in the Middle Fisher River Watershed in the Piedmont Region, North Carolina, USA. The 27-m riparian zone is located adjacent to a fertilized agricultural field planted with a rotation of corn and soybeans. Fertilizer was primarily applied as poultry litter in February and March. Due to intensive agriculture in the section of the watershed upstream of our study reach, the stream had straightened, was overly incised, and experienced abnormally high sediment loads. Consequently, the site was restored in 2012 using a Natural Channel Design (NCD) approach.[37] Restoration entailed the installation of cross-vanes – channel spanning boulder structures – to reduce erosion and create step-pool-riffle geomorphology. As part of restoration activities, the riparian zone was also regraded for an approximately 5 m zone extending out from the edge of the channel to create an inset floodplain, which entailed removal of vegetation and topsoil. Following regrading, the riparian zone was re-vegetated using a combination of seeding of herbaceous vegetation and live stakes of deciduous trees. Riparian zone soil is primarily sandy clay. Land use in the 1.43 km^2 drainage area is 54% agricultural (row crops [corn, soybean, and alfalfa], hay, and pasture), 26% forested, 14% herbaceous, 5% developed land, and 1% open space composed mainly of lawns, parks, and golf courses.

Site Instrumentation

The site was instrumented with a network of in-stream and riparian piezometers (Fig. 1a). In the riparian zone, 10 nests of piezometers were installed, containing 2-3 piezometers with 20 cm screens and one well at various depths. Piezometers were installed to approximately 50 cm depth increments until refusal in the field to a maximum depth of 275 cm below ground surface. Piezometers and wells were constructed from 1.27 cm and 5.1 cm inner diameter (ID) polyvinyl chloride (PVC) pipe, respectively. At each riparian piezometer nest, a static chamber was installed for measuring greenhouse gas fluxes at the soil-atmosphere interface. The static chamber was a PVC container 37 cm high and 27 cm in diameter. It was inserted 10 cm into the ground. Piezometer nest locations and site topography were surveyed using a Trimble M1 total station (Westminster, CO; Fig. 1a). Continuous HOBOware water level loggers (model #U20-001-02-Ti, Onset Computer Corporation, Bourne, MA), which recorded water levels every 15 minutes, were installed in a 5.1 cm slotted PVC pipe in the upper riparian zone and in an in-stream pool. A corresponding HOBOware smart barometric pressure datalogger (model #S-BPB-CM50) was installed in the upper riparian zone to complete pressure correction.

The site was also instrumented with an AcuRite precipitation gage (Primex Family of Companies, Geneva Lake, WI) to measure precipitation depth. Daily precipitation data was downloaded from National Oceanic and Atmospheric Administration (NOAA) for use in antecedent precipitation calculations.[38] Because 15-minute interval precipitation data was not available from NOAA, we also downloaded continuous rainfall data from Weather Underground (station ID: KNCDOBSO3, Fisher

Park, located 4.5 km south of the field site) to create continuous precipitation hyetographs.[39]

Hydrology and Biogeochemistry Methods

Hydrology and water chemistry were assessed once for baseflow conditions (7/1/15; Fig 1b) and at 24 and 72 hours following precipitation events for three storms of different magnitudes (1.65, 3.15, and 6.35 cm) during the summer of 2015 (Fig. 2). Representative summer baseflow hydrologic conditions were measured following 3 days with no rainfall. During baseflow and post-storm sampling, water level was measured manually in each piezometer using a Solinst Model 102M Mini Water Level Meter (Solinst, Gerogetown, ON). Following water level measurements, water samples were extracted from each riparian and stream piezometer and well and collected in acid-washed 140-mL polypropylene sample cups. A water sample was also collected from the stream. Wells and piezometers were capped between sampling events. At each site, saturated hydraulic conductivity was also measured, following Freeze and Cherry 1979.[40]

Water samples were transported to the laboratory on ice in a cooler. Water samples were filtered within 24 hours using 0.7 mm Whatman GF/F filters (Whatman, Inc., Florham Park, NJ) and frozen until analysis. Samples were analyzed for NO_3^-, ammonium (NH_4^+), and orthophosphate (PO_4^{3-}) using a SEAL AQ2 Discrete Analyzer (SEAL Analytical, Inc. Mequon, WI). Concentrations of NO_3^--N, NH_4^+-N, and PO_4^{3-}-P were determined using cadmium reduction (AQ2 Method EPA-114-A), the phenol method (AQ2 Method EPA-103-A), and ascorbic acid method (AQ2 EPA-118-A*),* respectively.[41-43] Dissolved organic carbon (DOC) and total dissolved nitrogen (TDN)

were determined on a Shimadzu Total Organic Carbon Analyzer with TNM attachment (Shimadzu Inc., Kyoto, Japan) via high-temperature combustion.

During greenhouse gas sampling, an airtight lid containing a sampling septum was installed on each chamber.[44] Five 15-mL headspace samples were collected in 30-mL syringes at 20-minute intervals over an 80-minute timespan. Samples were stored in 10 mL pre-evacuated vials. At the time of gas sampling, soil temperature was obtained via an Oakton Acorn Thermocouple Digital Thermometer (model # 2630650, Hach, Loveland, CO, USA) in the top 5-10 cm of the soil profile. Soil cores (approximately 30 cm^3) were collected in the top 5 cm of soil adjacent to the flux chamber to determine volumetric soil moisture in the laboratory by obtaining the difference in field-moist versus dried soil weight (72 hours in the drying oven at 60^{o}C).

Greenhouse gas sample analysis was completed within two weeks of collection. Concentrations of CO_2, CH_4, and N_2O were determined using a Shimadzu GC-2014® gas chromatograph (Shimadzu Corporation, Kyoto, Japan) equipped with a flame ionization detector (FID) and an electron capture detector (ECD) interfaced with a CombiPal autosampler (LEAP Technologies, Carrboro, NC). Greenhouse gas fluxes were computed as the change in concentration of gas over time multiplied by the chamber volume divided by soil area.[45] Greenhouse gases were also expressed in terms of 100-year CO_2 equivalent global warming potential, which entailed multiplying the mass of the gas by the global warming potential for each gas over 100 years (298 for N_2O and 25 for CH_4).[46]

Mapping and Statistical Analysis Methods

Maps of riparian groundwater height were created in Grapher (Version 10, Golden Software, Golden, CO). Hydraulic head was calculated as the sum of elevation head and pressure head at each piezometer location above a datum. Lateral hydraulic gradients through the riparian zone were determined via the change in hydraulic head over the distance between piezometers in the cross-section, while groundwater flow was calculated using the one-dimensional form of Darcy's Law.[47]

Analysis of riparian zone GHGs and water chemistry involved splitting the riparian area into two zones – "near stream" (NS; regraded inset floodplain) and "upper riparian zone" (UP; mid and near-field riparian piezometers). Each of these zones contained 5 nests of piezometers, with 5 associated static chambers (Fig. 1a). Nutrient percent removal (removal efficiency) was calculated by subtracting average near-stream nutrient concentrations from average upper riparian nutrient concentrations, dividing by average upper riparian nutrient concentration, and multiplying by 100.[48-50] Normality of data was tested via the Shapiro-Wilk W test[51]; distributions of all GHG and water chemistry data in both near-stream and upper riparian locations were determined to be non-normal. Therefore, nonparametric Kruskal-Wallis H tests and post-hoc Wilcoxon tests[52] were conducted to determine differences in GHG and dissolved solute concentrations in the near-stream and upper riparian zones between time points (24-72 hours) following each storm event and baseline conditions. Spearman's rho (r_s) correlation coefficients[53] were used to determine the strength and direction of monotonic relationships between GHG concentrations, water chemistry, environmental parameters (soil moisture, water table height, soil temperature) and storm magnitude. When conducting Spearman's rho correlation analysis, one measurement for each nest was used

(e.g., all water chemistry data from piezometers at each nest was averaged and included as one value in the correlation); samples were treated as randomized for the purpose of this analysis. Soil moisture distributions were normal; Analysis of Variance (ANOVA) and Tukey post-hoc tests were used to evaluate differences in soil moisture between post-storm periods. Linear regression was used to describe relationships between soil moisture and biogeochemical parameters. Statistical analyses were completed in JMP (SAS Institute Inc., Cary, NC), while graphics were created using Grapher (Version 10, Golden Software, Golden, CO) and SigmaPlot 11 (Systat Software, San Jose, CA).

Results

Hydrology

Baseflow stream stage from June through the beginning of July was generally 0.17 to 0.18 m (Fig. 2). During storms 1 and 2, stream water levels rose to 0.68 m and 0.48 m at peak flow, respectively. Storms 1 and 2 also produced riparian water table hydrographs that peaked 5 cm or less from the ground surface. Conversely, during storm 3, negligible changes in water table depth were observed in the riparian zone. Instead, riparian water table levels rose gradually with stream levels in the following two days, indicating a delayed groundwater response (Figs. 2 and 3).

Rainfall characteristics, as displayed in the hyetograph (Fig. 2), and antecedent conditions influenced these observed riparian and stream hydrograph responses. Rainfall during storm 1 was of moderate intensity (maximum: 3 mm hr^{-1}, average 1.23 mm hr^{-1}) and duration (approx. 35 hours), for a total of 3.15 cm of rain (Table 1), which led to synchronous stream and riparian zone peaks in stage (Fig. 2). Though storm 1 did not

have the highest magnitude, it did have the highest 14-d antecedent rainfall (10.46 cm), leading to the highest average water table height across the riparian zone at 24 hours following storm 1 (Fig. 3). Storm 1 produced the highest riparian hydraulic gradient and greatest groundwater flux (Table 2). Water table mounding was also most pronounced at nest 7 following storm 1 (Fig. 3a-b).

Storm 2 demonstrated higher total rainfall (6.35 cm; Table 1) but had a lower intensity (maximum: 2.3 mm hr^{-1}, average: 0.62 mm hr^{-1}) and longer duration (approx. 82 hours), producing multiple smaller peaks in the stream hydrograph (Fig. 2). The riparian hydrograph for this storm also presented a similar 2-peak pattern, with a much larger second peak. Storm 3 was the storm with the highest maximum and average intensity (5.1 mm hr^{-1} and 2.4 mm hr^{-1}) but was short duration (2 hours) and low magnitude (1.65 cm; Table 1). This storm, which produced a small stream peak and no riparian response at the location of the water level logger (Fig. 2), occurred latest in the season, in mid-July, and had the lowest 14-d antecedent rainfall conditions (6.90 cm). Riparian water table height, hydraulic gradient, and groundwater flux was lowest following storm 3 (Fig. 3, Table 2).

Water table height generally increased with increasing precipitation (Fig. 1b, 2, and 3). Soil moisture was significantly ($p<0.05$, ANOVA) higher than baseline conditions at all post-storm time points. Variation in soil moisture responses at 24 and 72 hours post-storm occurred with storm event magnitude (1.65 cm, 3.15 cm, and 6.35 cm) and duration (Table 1). Though variation in soil moisture was observed over time, soil moisture was consistently higher in the near-stream regraded inset floodplain (NS) than in the upland riparian section (UP) during both time periods (24 and 72 hours) after all storm events.

Riparian Water Chemistry

Following storm 1 (sample dates: 6/10/15-6/12/15), agricultural field edge (nest 1 and nest 6) NO_3^- concentrations were the highest post-storm (median: 24.2 mg N L^{-1}), driving the elevated median upper riparian NO_3^- concentrations (12.52 mg N L^{-1}, Fig. 4b). Upper riparian median NO_3^- concentrations were significantly lower following storm 2 and storm 3 than concentrations measured following storm 1 (1.46 and 0.88 mg N L^{-1} and $p = 0.0007$ and $p < 0.0001$, storms 2 and 3, respectively [Kruskal-Wallis and Wilcoxon post-hoc]). Despite differences in upper riparian NO_3^- concentrations, NO_3^- removal capacity of the riparian zone remained consistently high, ranging from 89-96% (Table 2). Near-stream mean NO_3^- concentrations (0.3 to 0.8 mg N L^{-1}) were low across storms, time points, and baseflow conditions (Fig. 4a). Total dissolved nitrogen concentrations followed a similar pattern, with high TDN in the upper riparian zone and lower TDN concentrations near-stream (Fig. 4c-d).

In the upper riparian zone, SRP was higher following storm 1 than for baseflow conditions, storm 2 and storm 3 (Fig. 4f, $p = 0.0002$, 0.0228 and <0.0001, respectively). Differences in SRP between storms occurred in the near-stream zone (Kruskal-Wallis H test, $p<0.0001$); SRP was significantly higher at 24 hours post-storm 1 and 72 hours post storm 3 than for all other time points (Fig. 4e). However, a much wider range of SRP removal (9 to 89%) than NO_3^- removal was observed (Table 2). SRP removal rates over 80% were associated with intermediate groundwater fluxes (6.4 to 8.2 L d^{-1}).

In the near-stream zone, a positive linear correlation was observed between SRP concentration and soil moisture ($R^2 = 0.16$, $p = 0.0179$). Over the whole riparian zone,

SRP concentration was correlated to water table height ($r_s = 0.28$, $p = 0.0177$). A significant positive relationship also existed between SRP concentration and N_2O flux ($r_s = 0.43$, $p = 0.0002$; Table 3).

Greenhouse Gas Fluxes

Though CO_2 emissions in both the near-stream and upper riparian zone following storm events were comparable to representative background fluxes, shifts in consumption-emission dynamics relative to baseflow sampling occurred for both CH_4 and N_2O fluxes (Fig. 5). Values above "0" indicate GHG emission is occurring from riparian soils (source), while values below "0" represent GHG consumption (sink). In terms of N_2O, the upper (UP) riparian zone shifted from sink to source following all three storms as compared to baseflow conditions. However, the source strength varied between storms; emissions were significantly higher (Kruskal-Wallis H test, p=0.02) 24 hours post-storm 1 than during both 24 and 72 hours post-storm 3 (Fig. 5b, Wilcoxon post hoc, p=0.0122 and 0.0122, respectively). The near-stream riparian zone served as a weak source (e.g., storm 2, 24 hours) or as a sink for N_2O (e.g., storm 2, 72 hours, Fig. 5a).

The near-stream (NS) riparian zone exhibited a shift in sink to source for CH_4. The storm with the greatest precipitation (storm 2) had the greatest mean CH_4 flux at 24 hours post-storm (42 mg C m^{-2} d^{-1}) compared to other storms (range of means at other time points: -18 to 9 mg C m^{-2} d^{-1}), though this difference was not statistically significant (Fig. 5c). The mean value was driven by a hot spot of CH_4 release at nest 8, and the median was lower, at 8.8 mg C m^{-2} d^{-1}. Conversely, the upper riparian zone often served as a sink for CH_4 (Fig. 5d).

Changes in water chemistry, water table height, and storm magnitude correlated to GHG fluxes. Across the riparian zone, N_2O emissions were significantly correlated to TDN and NO_3^- concentrations (Spearman's rank; TDN: $r_s = 0.44$, $p = 0.0002$, and NO_3^- : $r_s = 0.47$, $p < 0.0001$) and water table height ($r_s = 0.35$, $p = 0.0025$) (Table 3). A significant inverse relationship between N_2O and CH_4 emissions was also observed ($r_s = -0.24$, $p = 0.0470$). Overall, CO_2 flux decreased with increasing storm magnitude ($r_s = -0.26$, $p = 0.0279$) (Table 3).

When expressed in total CO_2 equivalents (CO_{2eq}), CO_2 comprised the majority of CO_{2eq} GHG emissions in the riparian zone (Fig. 6a). At baseflow conditions, N_2O contributions to average riparian GHG emissions were negligible in the near-stream (0.02% of CO_{2eq}) and upper riparian zones (-0.05%). Both the upper riparian zone and near-stream zone were methane sinks at baseflow conditions (< -0.5% and < -12.9% of CO_{2eq}, respectively). However, during some post-storm time points, both N_2O and CH_4 became larger contributors to CO_{2eq}. In the upper riparian zone, N_2O contributed 6-10% of GHG emissions following storm 1 (24 hours = 9.10%, 72 hours = 7.98%) and storm 2 (72 hours = 6.01%) (Fig. 6b). In the near-stream zone, CH_4 emissions contributed to 27% of the CO_{2eq} at 24 hours post-storm 2 and 5% of CO_{2eq} at 72 hours following storm 3 (Fig. 6c). Highest absolute GHG flux (in terms of CO_{2eq}) occurred 24 hours following storm 3, though on a statistical basis, this time point was not significantly different. At this time point, CO_2 emissions comprised the majority of CO_{2eq}, as net riparian CH_4 emissions were negative and N_2O emissions were less than 1% of CO_{2eq}. Overall, net riparian GHG emissions at baseflow conditions and following storms were positive.

Discussion

Impact of Storm Characteristics and Antecedent Precipitation on Site Hydrology

Both antecedent conditions and precipitation characteristics (intensity, duration, and magnitude) influenced riparian water table response, hydraulic gradient, and groundwater fluxes. Though storm 1 was of intermediate magnitude (3.15 cm), it had the highest 14-d antecedent rainfall and the hyetograph had a pronounced peak. Following this storm, average riparian water table height and near-stream soil moisture were higher than for all other storm observations at 24-hours post-storm. Groundwater mounding also occurred, which is consistent with other studies demonstrating groundwater mounding following rapid rises in water table.[55,56] Though the precipitation amount for storm 2 was 6.35 cm, the rainfall was widely distributed over the course of a few days, which led to multiple peaks in the riparian hydrograph. The rapid occurrence of the second, larger peak, which rose disproportionally to precipitation inputs, was expected based on capillary action, as the water table was elevated from the first hydrograph peak.[57]

Conversely, storm 3, which had the lowest recorded total rainfall amount and lowest 14-d antecedent precipitation, had virtually no response in the riparian hydrograph due to a lower pre-storm water table. Storm 3 occurred in mid-July, during a time of water table recession. Water table drawdown at this time was likely occurring in response to warmer temperatures, increased evapotranspiration, and drainage to the stream. Groundwater fluxes and water table height were lower than baseflow conditions following storm 3, which is consistent with studies demonstrating the large impact dry antecedent moisture conditions may have on riparian hydrology and connectivity.[58]

Within this sampling period, storms above 3 cm that had 14-d antecedent rainfall amounts of over 7 cm elicited a strong riparian groundwater table rise while other storms did not. This suggests further study of temporal changes of riparian water table response in agricultural Piedmont riparian zones is necessary to understand conditions under which water tables rise disproportionately to precipitation input. Though Macrae *et al.* (2010) describe a precipitation threshold for catchment hydrologic response, they note hydrologic responses are often variable and non-linear, meriting further study.[59]

Impact of Storm Intensity and Antecedent Precipitation on Nutrient Chemistry

High agricultural field edge and upper riparian NO_3^- concentrations which occurred at the beginning of the summer season likely represented export of NO_3^- that had accumulated on the field and in groundwater via nitrification during the late spring/early summer period. Other studies have demonstrated NO_3^- may accumulate during dry periods and a flushing effect may occur during wetter conditions following storm events.[60-62] Following storm 2, dilution began to occur as NO_3^- was flushed out of the system, culminating in lowest near-field NO_3^- concentrations following the final storm measured in the season, storm 3. A similar export-dilution pattern was observed with TDN and NH_4^+ (ammonium data not shown). Despite the elevated near-field NO_3^- concentrations, riparian N removal remained high following all storms. This is consistent with other studies in North Carolina showing high NO_3^- removal (> 90%) in riparian zones, even when high field edge NO_3^- concentrations (> 5 mg N L^{-1}) are observed.[63-65]

Our results indicate that at our field site, hot moments of nitrogen export deliver nitrogen to subsurface hot spots of nitrogen processing. Other studies have shown that

hydrologic flowpaths may bypass areas of riparian zones that may facilitate denitrification and suggest hydrologic alteration of sites to achieve effective nitrate removal.[9,66] Previous research at our field site, which includes a regraded riparian zone, has shown that denitrification potential is higher in the regraded riparian bench than in-stream.[67] This suggests that enhanced stream-riparian interactions through stream bank regrading may play a key role in overall NO_3^- removal following storms. Other research has demonstrated that restored inset floodplains remove more N than naturalized floodplains following storm-induced inundation events.[68] Additionally, studies have shown that post-storm denitrification rates in restored floodplains may be higher than those in wetlands,[69] and that restored connected stream banks that promote flooding following storm events have higher denitrification rates than restored unconnected stream banks.[70] This indicates cumulative impacts of restoration design and storm characteristics may influence the degree of nitrate removal or export.

Soluble reactive phosphorus retention was more variable, ranging from negligible removal (9%) during storm 3 to high removal (89%) 72 hours after storm 2. Other studies have reported high variability in SRP removal in riparian zones, with some sites reported to be sources of SRP to the stream (negative removal) and other moderate sinks (50% removal).[71] In the stream, high SRP concentrations (> 0.1 mg L^{-1} and 0.25 mg L^{-1}) were observed following storm 1 and storm 3, respectively. This is consistent with the release of SRP from agricultural soil to the stream due to seasonal soil saturation, flooding, and high precipitation magnitude.[72-74]

Impact of Storm Intensity and Antecedent Precipitation on GHG Dynamics at the Soil-Atmosphere Interface

Shifts in summer season GHG source-sink dynamics occurred following storm events; the upper riparian zone shifted from a sink to source of N_2O and the near-stream zone shifted from a sink to source of CH_4. Shifts in riparian and wetland source-sink dynamics following shifts in soil conditions have been similarly reported in the literature. Jacinthe *et al.* (2015) describe a shift in sink to source CH_4 behavior in a low-lying section of an agricultural riparian zone following a flooding event[75], while Teiter and Mander (2005) describe conditions under which riparian zones and wetlands exhibit various sink-source behavior in CH_4 and CO_2 emissions as a function of water table height and soil oxic status.[76] This research agrees with previous work at our field sites in North Carolina, which has shown antecedent watershed conditions and restoration status influence magnitude and type of GHG release following storms.[77] In water-limited environments (often unrestored riparian zones), large fluxes of CO_2 dominate following storm events, however, CH_4 and N_2O release occurs in restored riparian saturated soils as shifts in redox conditions occur following post-storm water table fluctuations.[77]

Storm timing and magnitude also influenced the magnitude of GHG emissions. For example, N_2O fluxes were significantly higher at 24 hours post-storm 1 than at either the 24 or 72 hour time points following storm 3. Storm 1 occurred earliest in the summer season, had the greatest antecedent precipitation, had pronounced peaks in stream and riparian hydrographs, and was larger in magnitude than storm 3. These factors likely led to a smaller subsidy of NO_3^- available for storm 3 at the field edge, since near-field soil flushing occurred following storms 1 and 2. Lower N_2O fluxes were likely observed due

to the lack of N source for nitrification and denitrification, evidenced by lower NO_3^- concentrations, and lack of prolonged anoxia, evidenced by lower water table height. Storm 3 also had the lowest antecedent precipitation and groundwater rise, indicating a water-limited environment. Post-storm 3, CO_2 emissions were highest, though not significantly. Based on this study, storm timing, magnitude, and antecedent conditions are important for predicting riparian nutrient dynamics and GHG response.

Integrating Riparian Biogeochemistry Results in the Context of Thermodynamics

Overall, our results agree with the current scientific understanding of riparian biogeochemistry, as thermodynamics dictates oxidation-reduction dynamics based on energetically-favorable microbially-mediated reactions.[78] However, though field observations agree with thermodynamics, storm characteristics influence site hydrology, leading to differences in biogeochemical response. Figure 7 integrates these proof-of-concept findings into a conceptual illustration, including antecedent conditions and storm characteristics, that lead to different biogeochemical responses. This diagram provides a visual assessment of when biogeochemical hot moments may occur, across a gradient of storm timing, duration, magnitude, and intensity (panel a). Panel b contains a visualization of where hot spots of biogeochemical release may occur on the landscape.

Following storm events, water table height and soil moisture increase, leading to an increase in microbial metabolism and CO_2 release in this water-limited environment.[79] In this study, a storm event of high intensity and low duration and magnitude which occurred following dry antecedent conditions in a water-limited riparian zone had the greatest overall riparian GHG emissions in terms of CO_{2eq} (Figs. 6 and 7). Other studies

conducted in riparian zones in the southern United States have demonstrated pulses of CO_2 release occur following precipitation events in water-limited environments [18,20,80] and that riparian zones located near agricultural activities have larger rates of CO_2 exchange than unimpacted riparian zones.[81] The negative correlation between CO_2 emissions and precipitation magnitude in this study indicates that production of CO_2 may decline as the local environment becomes non-water-limited.[82]

Following CO_2 release, oxygen content in soils may decrease as water continues to fill pore spaces and denitrification occurs in the presence of NO_3^- (electron acceptor) and organic carbon (electron donor). As water tables recede, denitrification may not progress to completion (i.e., production of N_2 gas) as soil pore spaces fill with O_2, and N_2O, a byproduct of denitrification, is released.[18,28] Large fluxes of N_2O in the upper riparian zone occurred following the storm closest to fertilizer application, a storm of intermediate magnitude and intensity with high near-field NO_3^- concentrations (Fig. 7). This study identified dissolved nitrogen (NO_3^- and TDN) and water table height as important drivers of N_2O fluxes (Table 3). Though high N_2O fluxes occurred, denitrification lead to high riparian zone NO_3^- removal.

Following denitrification, release of SRP may occur in inundated floodplain soils via mobilization from upper soil horizons or reduction of P-bound iron under reducing conditions.[83-85] In this study, low SRP removal was observed following storm 3, following high CO_2 release. High near-stream SRP concentrations were also observed following storm 1, concurrent with high NO_3^- removal and upland N_2O release. SRP was positively correlated to N_2O, water table height, and soil moisture (Table 3). Other restored floodplains, which experience frequent hydrologic fluctuations due to landscape

setting, have demonstrated phosphorus mobilization and export.[86,87] Flushing of near-stream SRP and erosion of sediments, which may release sorbed particulate P into solution, may create pollutant problems in downstream waters.[9]

Finally, CH_4 release has been shown to be driven by local soil water content.[88] Methanogenesis occurs during prolonged anoxic conditions, often in low-lying, flooded areas with high soil moisture (such as restored backswamps,[89] riparian floodplain wetlands,[18,90] kettle holes,[91] and freshwater fens[92]). In this study, as the storm with the greatest duration and highest magnitude had the greatest CH_4 release (albeit not significantly, Fig. 7); CH_4 comprised up to 26.7% of total near-stream GHG emissions (in CO_{2eq}) following storm 2 as the inset floodplain remained saturated. Adherence to thermodynamic principles was demonstrated via an inverse relationship between N_2O and CH_4 release (Table 3). Merbach et al. (2002) showed higher water levels lead to dampened N_2O response and enhanced CH_4 release, while Bonnet *et al.* (2013) described inhibition of CH_4 by NO_3^- and N_2O during flooding events.[91,93] However, for other storms and time points, CH_4 production was negligible or negative. Although saturated inset floodplains function similarly to wetlands as hot spots for CH_4 release, typically CO_{2eq} is dominated by CO_2 in other settings, such as forested riparian zones.[94,95]

Conclusion

This research stresses the need to continue developing conceptual models of systematic riparian biogeochemical behavior following storms of various timings and magnitudes to provide direction for watershed managers and restoration practitioners who aim to reduce potential pollutant tradeoffs in the context of local climatic conditions.

Though riparian N removal remained high throughout the study, this removal occurred at the expense of CO_2 release (storm 3), N_2O release (storms 1 and 2), CH_4 release (storm 2) and low SRP retention (storms 1 and 3), through possible mechanisms described above. Though restored riparian floodplains attenuate flow, increase residence times, and reduce export of suspended solids, particulate phosphorus, and dissolved nitrogen,[96-98] pollutant tradeoffs may exist in terms of GHG release and SRP mobilization.

Although more studies need to be conducted on dynamics of multiple water and air contaminants of concern following storms, we propose that the conceptual diagram depicted here (Fig. 7) can be a useful starting point to illustrate the complexities that exist within one riparian zone under a range of hydroclimatic conditions when planning watershed restoration projects. Though this research shows one riparian zone can have different biogeochemical responses for three different storm types, all possible storm types were obviously not represented in this study (e.g., high magnitude, high intensity, high duration). Directly pertinent to this point from a management perspective, Moorhead *et al.* (2008) recommend comprehensive pre and post-restoration hydrologic assessment to account for rainfall variability.[99] In particular, we argue that due to spatial and temporal variability in environmental drivers of GHG fluxes and nutrient retention and release, it is important to continue investigating riparian biogeochemistry during times of varying soil moisture and water table height following storm events of different magnitudes. Others have recognized the importance of examining the effectiveness of restoration projects during large storms.[100] Developing protocols for monitoring riparian zone hydrology and biogeochemistry following storms will be an essential component of

restoration monitoring, assessment, and design, as climate change continues to alter precipitation patterns.

Conflicts of Interest

There are no conflicts of interest to declare.

Acknowledgements

This work was supported by the United States Department of Agriculture – Agriculture and Food Research Initiative [Award # 2012-67019-30226] and the National Science Foundation Graduate Research Fellowship Program [Award # 1439650]. Thanks are due to the Surry County Soil and Water Conservation District, especially Greg Goings, for granting access to the site for the duration of the study. We thank Jordan Martin-Gross, Sara Marchese, Obed Varughese, Gavin Downs, Laura Maria Ortiz de Zarate, and Mandy Limiac for aid in site instrumentation, sampling, and laboratory analysis.

References

1 P.M. Vitousek, J.D. Aber, R.W. Howarth, G.E. Likens, P.A.Matson, D.W. Schindler, W.H. Schlesinger and D.G. Tilman, Human alteration of the global nitrogen cycle: sources and consequences, *Ecol. Appl.,* 1997, **7**, 737-750.
2 N. Rabalais, Nitrogen in aquatic ecosystems, *AMBIO: J. Human Environ*, 2002, **31**, 102-112.
3 L.B.M. Vought, J. Dahl, C. L. Pedersen and J.O. Lacoursiere, Nutrient retention in riparian ecotones, *Ambio*, 1994, 342-348.
4 M.G. Dosskey, P. Vidon, N.P. Gurwick, C.J., Allan, T.P. Duval, and R. Lowrance, The role of riparian vegetation in protecting and improving chemical water quality in streams, JAWRA *J. Am. Water Res. Assoc.*, 2010, *46*, 261-277.
5 L.L. Osborne and D.A. Kovacic, Riparian vegetated buffer strips in water-quality restoration and stream management, *Freshwater Biol.,* 1993, **29**, 243-258.

6 C.C. Hoffmann, C. Kjaergaard, J. Uusi-Kämppä, H.C.B Hansen, and B. Kronvang, Phosphorus retention in riparian buffers: review of their efficiency, *J. Environ. Qual.*, 2009, **38**, 1942-1955.
7 P.G. Vidon, M.K. Welsh and Y.T. Hassanzadeh, Twenty Years of Riparian Zone Research (1997–2017): Where to Next?, *J. Environ. Qual.*, 2018.
8 M.E. McClain, E.W. Boyer, C.L Dent, S.E. Gergel, N.B. Grimm, P.M. Groffman, S.C. Hart, J.W. Harvey, C.A. Johnston, E. Mayorga and W.H. McDowell, Biogeochemical hot spots and hot moments at the interface of terrestrial and aquatic ecosystems, *Ecosystems*, 2003, **6**, 301-312.
9 P. Vidon, C. Allan, D. Burns, T.P. Duval, N. Gurwick, S. Inamdar, R. Lowrance, J. Okay, D. Scott, and S. Sebestyen, Hot spots and hot moments in riparian zones: potential for improved water quality management, *JAWRA J. Am. Water Res. Assoc.*, 2010, **46**, 278-298.
10 P.G. Vidon and A.R. Hill, Landscape controls on nitrate removal in stream riparian zones, *Water Resour. Res.*, 2004, **40**.
11 K.-H. Lee, T. M. Isenhart and R. C. Schultz, Sediment and nutrient removal in an established multi-species riparian buffer, *J. Soil Water Cons.*, 2003, **58**, 1–8.
12 T. P. Burt, G. Pinay, G. F. E. Matheson, N. E. Haycock, A. Butturini, J. C. Clement, S. Danielescu, D.J. Dowrick, M.M. Hefting, A. Hillbricht-Ilkowska, and V. Maitre, Water table fluctuations in the riparian zone: comparative results from a pan-European experiment, *J. Hydrol.,* 2002, **265**, 129-148.
13 S. Sabater, A. Butturini, J.C. Clement, T. Burt, D. Dowrick, M. Hefting, V. Matre, G. Pinay, C. Postolache, M. Rzepecki, and F. Sabater, Nitrogen removal by riparian buffers along a European climatic gradient: patterns and factors of variation, *Ecosystems*, 2003, **6**, 0020-0030.
14 A.A. Tomasek, M. Hondzo, J.L. Kozarek, C. Staley, P. Wang, N. Lurndahl, and M.J. Sadowsky, Intermittent flooding of organic-rich soil promotes the formation of denitrification hot moments and hot spots, *Ecosphere*, 2019,**10**, e02549.
15 G.W. Raisin, D.S. Mitchell, and R.L. Croome, The effectiveness of a small constructed wetland in ameliorating diffuse nutrient loadings from an Australian rural catchment, *Ecol. Eng.*, 1997, **9**, 19-35.
16 D.F. Finkand and W.J. Mitsch, Seasonal and storm event nutrient removal by a created wetland in an agricultural watershed, *Ecol. Eng.*, 2004, 23, 313-325.
17 S.S. Kaushal, P.M. Mayer, P.G. Vidon, R.M. Smith, M.J. Pennino, T.A. Newcomer, S. Duan, C. Welty and K.T. Belt, Land use and climate variability amplify carbon, nutrient, and contaminant pulses: a review with management implications, *J. Am. Water Res. Assoc.*, 2014, **50**, 585–614.
18 P. Vidon, P.-A. Jacinthe, X. Liu, K. Fisher and M. Baker, Hydrobiogeochemical controls on riparian nutrient and greenhouse gas dynamics: 10 years post-restoration, *J. Am. Water Res. Assoc.*, 2014, **50**, 639–652.
19 S. Poblador, A. Lupon, S. Sabaté, and F. Sabater, Soil water content drives spatiotemporal patterns of CO_2 and N_2O emissions from a Mediterranean riparian forest soil, *Biogeosciences*, 2017, **14**, 4195-4208.
20 T. K. Harms and N. B. Grimm, Responses of trace gases to hydrologic pulses in desert floodplains, *J. Geophysical Res.: Biogeosciences,* 2012, **117**, 1-14.

21 E. Leon, R. Vargas, S. Bullock, E. Lopez, A.R. Panosso and N. La Scala Jr., Hot spots, hot moments, and spatio-temporal controls on soil CO_2 efflux in a water-limited ecosystem, *Soil Biol. Biochemistry*, 2014, **77**, 12-21.
22 P. Vidon, S. Marchese, M. Welsh and S. McMillan, Impact of precipitation intensity and riparian geomorphic characteristics on greenhouse gas emissions at the soil-atmosphere interface in a water-limited riparian zone, *Water, Air, Soil Pollution,* 2016, **227**, 1-12.
23 J. Jauhiainen, H. Takahashi, J. E. Heikkinen, P.J. Martikainen and H. Vasander, Carbon fluxes from a tropical peat swamp forest floor, *Global Change Biol.*, 2005, **11**, 1788–1797.
24 Ü. Mander, M. Maddison, K. Soosaar and K. Karabelnik, The impact of pulsing hydrology and fluctuating water table on greenhouse gas emissions from constructed wetlands, *Wetlands*, 2011, **31**, 1023–1032.
25 C.J. Talbot, E.M. Bennett, K. Cassell, D.M. Hanes, E.C. Minor, H. Paerl, P.A. Raymond, R. Vargas, P.G. Vidon, W. Wollheim, and M.A. Xenopoulos, The impact of flooding on aquatic ecosystem services, *Biogeochemistry*, 2018, **141**, 439-461.
26 J.E. McLain and D.A. Martens, Moisture controls on trace gas fluxes in semiarid riparian soils, *Soil Sci. Soc. Am. J.,* 2006, **70**, 367-377.
27 P.G. Vidon, Not all riparian zones are wetlands: Understanding the limitation of the wetland bias problem, *Hydrol. Process*., 2017, **31**, 2125-2127.
28 P.A. Jacinthe, J.S. Bills, L.P. Tedesco and R.C. Barr, Nitrous oxide emission from riparian buffers in relation to vegetation and flood frequency, *J. Environ. Qual.*, 2012, **41**, 95–105.
29 E. Samaritani, J. Shrestha, B. Fournier, E. Frossard, F. Gillet, C. Guenat, P. A. Niklaus, K. Tockner, E.A.D. Mitchell, and J. Luster. Heterogeneity of soil carbon pools and fluxes in a channelized and a restored floodplain section (Thur River, Switzerland). *Hydrol. Earth System Sci. Discussions*, 2011, **8**, 1059-1091.
30 G. Bullinger-Weber, R.C. Le Bayon, A. Thébault, R. Schlaepfer, and C. Guenat, Carbon storage and soil organic matter stabilisation in near-natural, restored and embanked Swiss floodplains, *Geoderma*, 2014, **228**, 122-131.
31 J. Kauffman, R.L. Boone, N.O. Beschta, and D. Lytjen, An ecological perspective of riparian and stream restoration in the western United States, *Fisheries,* 1997*,* **22**, 12-24.
32 J.S. Bash and C.M. Ryan, Stream restoration and enhancement projects: is anyone monitoring?, *Environ. Manage.*, 2002, **29**, 877-885.
33 E.S. Bernhardt, E.B. Sudduth, M.A. Palmer, J.D. Allan, J.L. Meyer, G. Alexander, J. Follastad-Shah, B. Hassett, R. Jenkinson, R. Lave, J. Rumps, and L. Pagano, Restoring rivers one reach at a time: results from a survey of US river restoration practitioners, *Restoration Ecol.*, 2007, **15,** 482-493.
34 G.M. Lovett, D.A. Burns, C.T. Driscoll, J.C. Jenkins, M.J. Mitchell, L. Rustad, J.B. Shanley, G.E. Likens, and R. Haeuber, Who needs environmental monitoring?, *Front. Ecol. Environ.*, 2007*,* **5**, 253-260.
35 C. Weber, U. Åberg, A.D. Buijse, F.M.R. Hughes, B.G. McKie, H. Piégay, P. Roni, S. Vollenweider, and S. Haertel-Borer, Goals and principles for programmatic river restoration monitoring and evaluation: collaborative learning across multiple projects, *Wiley Interdisciplinary Reviews: Water,* 2018*,* **5**, e1257.

36 Z. Rubin, G. Kondolf, and B. Rios-Touma, Evaluating stream restoration projects: what do we learn from monitoring?, *Water*, 2017, **9**, 174.
37 D. L. Rosgen, Rosgen geomorphic channel design, *Stream Restoration Design Natl. Eng. Handb.*, 2007, **654**, 11-1 – 11-76.
38 National Oceanic and Atmospheric Administration National Centers for Climate Information: North Carolina. http://www1.ncdc.noaa.gov/pub/data/ghcn/daily. Accessed 5/26/2016.
39 Weather Underground: Dobson, NC, Station ID: KNCDOBSO3, Fisher Park https://www.wunderground.com/personal-weather-station/dashboard?ID=KNCDOBSO3. Accessed 5/26/2016.
40 Freeze, R. A., and J. A. Cherry (1979), Groundwater, Prentice-Hall, Old Tappan, N. J.
41 Standard Methods for the Examination of Water and Wastewater, 4500-NO3-F Cadmium Reduction Method, American Public Health Association.
42 US Environmental Protection Agency, Method EPA-103-A, US Government Printing Office, Washington, DC.
43 US Environmental Protection Agency, EPA-118-A , US Government Printing Office, Washington, DC.
44 P.-A. Jacinthe and W. A. Dick, Soil management and nitrous oxide emissions from cultivated fields in southern Ohio, *Soil Tillage Res.*, 1997, **41**, 221–235.
45 P.-A. Jacinthe and R. Lal, Effects of soil cover and land-use on the relations flux-concentration of trace gases, *Soil Sci.*, 2004, **169**, 243–259.
46 The United States Environmental Protection Agency, *Inventory of U.S. Greenhouse Gas Emissions and Sinks: 1990-2016,* EPA 430-R-18-003, 2017.
47 K.K. Watson, An instantaneous profile method for determining the hydraulic conductivity of unsaturated porous materials, *Water Resources Research*, 1966, **2**, 709-715.
48 M.M. Brinson, Changes in the functioning of wetlands along environmental gradients, *Wetlands*, 1993, **13**, 65-74.
49 A.R. Hill, Nitrate removal in stream riparian zones, *J. Env. Qual.*, 1996, **25**, 743-755.
50 P.M. Mayer, S.K. Reynolds, M.D. McCutchen, and T.J. Canfield, Meta-analysis of nitrogen removal in riparian buffers, *J. Environ. Qual.*, 2007, **36**, 1172-1180.
51 S.S. Shapiro and M.B. Wilk, An analysis of variance test for normality (complete samples), *Biometrika*, 1965, **52**, 591-611.
52 A. Vargha, and H.D. Delaney, The Kruskal-Wallis test and stochastic homogeneity, *J. Educational Behavioral Statistics*, 1998, **23**, 170-192.
53 T.D. Gautheir, Detecting trends using spearman's rank correlation coefficient. *Environ. Forensics*, 2001, **2**, 359-362.
54 P.A. Cook and P. Wheater. Using statistics to understand the environment. Routledge, 2005.
55 P. G. Vidon, Towards a better understanding of riparian zone water table response to precipitation: surface water infiltration, hillslope contribution or pressure wave processes, *Hydrol. Processes*, 2012, **26**, 3207–3215.
56 M. Jung, T. P. Burt and P. D. Bates, Toward a conceptual model of floodplain water table response, *Water Resour. Res.*, 2004, **40**, 1-13.

57 R. W. Gillham, The capillary fringe and its effect on water-table response, *J. Hydrol.*, 1984, **67**, 307–324.
58 S. K. McMillan, H. F. Wilson, C. L. Tague, D. M. Hanes, S. Inamdar, D. L. Karwan, T. Loecke, J. Morrison, S. F. Murphy and P. Vidon, Before the storm: antecedent conditions as regulators of hydrologic and biogeochemical response to extreme climate events, *Biogeochemistry*, 2018, 1–15.
59 M. L. Macrae, M. C. English, S. L. Schiff and M. Stone, Influence of antecedent hydrologic conditions on patterns of hydrochemical export from a first-order agricultural watershed, in Southern Ontario, Canada, *J. Hydrol.*, 2010, **389**, 101–110.
60 T.D. Loecke, A.J. Burgin, D.A. Riveros-Iregui, A.S. Ward, S.A. Thomas, C.A. Davis and M.A.S. Clair, Weather whiplash in agricultural regions drives deterioration of water quality, *Biogeochemistry*, 2017, **133**, 7–15.
61 D.B. Lewis and N.B. Grimm, Hierarchical regulation of nitrogen export from urban catchments: interactions of storms and landscapes, *Ecol. Appl.*, 2007, **17**, 2347–2364.
62 R. Jiang, K.P. Woli, K. Kuramochi, A. Hayakawa, M. Shimizu and R. Hatano, Hydrological process controls on nitrogen export during storm events in an agricultural watershed, *Soil Sci. Plant Nutrition*, 2010, **56**, 72–85.
63 J.W. Gilliam, R. B. Daniels and J. F. Lutz, Nitrogen Content of Shallow Ground Water in the North Carolina Coastal Plain, *J. Environ. Quality*, 1974, **3**, 147–151.
64 T.C. Jacobs and J.W. Gilliam, Riparian Losses of Nitrate from Agricultural Drainage Waters, *J. Environ. Qual.*, 1985, **14**, 472–478.
65 T.B. Spruill, Effectiveness of riparian buffers in controlling ground-water discharge of nitrate to streams in selected hydrogeologic settings of the North Carolina Coastal Plain, *Water Sci. Technol.*, 2004, **49**, 63–70.
66 T.P. Burt, L.S. Matchett, K.W.T. Goulding, C.P. Webster, and N.E. Haycock, Denitrification in riparian buffer zones: the role of floodplain hydrology, *Hydrol. Process.*, 1999, **13**, 1451-1463.
67 M.K. Welsh, S.K. McMillan and P.G. Vidon, Denitrification along the stream-riparian continuum in restored and unrestored agricultural streams, *J. Environ. Qual.*, 2017, **46**, 1010–1019.
68 B.R. Hanrahan, J.L. Tank, M.M. Dee, M.T. Trentman, E.M. Berg, and S.K. McMillan, Restored floodplains enhance denitrification compared to naturalized floodplains in agricultural streams, *Biogeochemistry*, 2018, **141**, 1-19.
69 S.S. Roley, J.L. Tank, and M.A. Williams, Hydrologic connectivity increases denitrification in the hyporheic zone and restored floodplains of an agricultural stream, *J. Geophysical Res.: Biogeosciences*, 2012, **117**, G3.
70 S.S. Kaushal, P.M. Groffman, P.M. Mayer, E. Striz and A.J. Gold, Effects of stream restoration on denitrification in an urbanizing watershed, *Ecol. Appl*., 2008, **18**, 789-804.
71 X. Liu, P. Vidon, P.-A. Jacinthe, K. Fisher and M. Baker, Seasonal and geomorphic controls on N and P removal in riparian zones, of the US Midwest, *Biogeochemistry*, 2014, **119**, 245–257.
72 J.T. Sims, R.R. Simard and B.C. Joern, Phosphorus loss in agricultural drainage: Historical perspective and current research, *J. Environ. Qual.*, 1998, **27**, 277–293.
73 Y.E.O and D.S. Ross, Phosphate release from seasonally flooded soils, *J. Environ. Qual.*, 2001, **30**, 91–101.

74 P. Vidon, H. Hubbard, P. Cuadra, and M. Hennessy, Storm phosphorus concentrations and fluxes in artificially drained landscapes of the US Midwest. *Agricultural Sciences*, 2012, **3**, 474.
75 P. A. Jacinthe, Carbon dioxide and methane fluxes in variably-flooded riparian forests, *Geoderma*, 2015, **241**, 41–50.
76 T. Sille and U. Mander, Emission of N_2O, N_2, CH_4, and CO_2 from constructed wetlands for wastewater treatment and from riparian buffer zones, *Ecol. Eng.*, 2005, **25**, 528–541.
77 P. G. Vidon, S. Marchese, M. K. Welsh and S. K. McMillan, Short-term spatial and temporal variability in greenhouse gas fluxes in riparian zones, *Environ. Monitoring Assessment*, 2015, **187**, 1-9.
78 L.O. Hedin, J.C. von Fischer, N.E. Ostrom, B.P. Kennedy, M.G. Brown and G.P. Robertson, Thermodynamic constraints on nitrogen transformations and other biogeochemical processes at soil–stream interfaces, *Ecology*, 1998, **79**, 684–703.
79 R. J. Naiman, H. Decamps and M. E. McClain, in *Riparia: Ecology, Conservation, Management Streamside Communities*, Elsevier, San Diego, 2010, ch. 4-5, pp. 79-158.
80 Liu, Ran, Ellen Cieraad, and Yan Li, Summer rain pulses may stimulate a CO_2 release rather than absorption in desert halophyte communities, *Plant Soil,* 2013, **373**, 799-811.
81 R.M. Petrone, P. Chahil, M.L. Macrae, and M.C. English, Spatial variability of CO_2 exchange for riparian and open grasslands within a first-order agricultural basin in Southern Ontario. *Agriculture, ecosystems & environment*, 2018, **125**, 137-147.
82 L. Xu, D.D. Baldocchi, and J. Tang, How soil moisture, rain pulses, and growth alter the response of ecosystem respiration to temperature, *Global Biogeochemical Cycles, 2004,* **18**.
83 D.S. Baldwin and A.M. Mitchell, The effects of drying and re-flooding on the sediment and soil nutrient dynamics of lowland river–floodplain systems: a synthesis, *Regulated Rivers: Research & Management: An International Journal Devoted River Research Management*, 2000, **16**, 457-467.
84 A. J. Burgin, W. H. Yang, S. K. Hamilton and W. L. Silver, Beyond carbon and nitrogen: how the microbial energy economy couples elemental cycles in diverse ecosystems, *Frontiers Ecol. Environ.*, 2011, **9**, 44–52.
85 R. Dupas, G. Gruau, S. Gu, G. Humbert, A. Jaffrézic, and C. Gascuel-Odoux, Groundwater control of biogeochemical processes causing phosphorus release from riparian wetlands, *Water Research*, 2015, **84**, 307-314.
86 M. Ardón, S. Montanari, J.L. Morse, M.W. Doyle and E.S. Bernhardt, Phosphorus export from a restored wetland ecosystem in response to natural and experimental hydrologic fluctuations, *J. Geophysical Res.: Biogeosciences,* 2010, **115**, G4.
87 B. W. Surridge, A. L. Heathwaite and A. J. Baird, Phosphorus mobilisation and transport within a long-restored floodplain wetland, *Ecol. Eng.*, 2012, **44**, 348–359.
88 K. E. Kaiser, B.L. McGlynn, and J.E. Dore, Landscape analysis of soil methane flux across complex terrain, *Biogeosciences,* 2018, **15**, 3143-3167.
89 J. Batson, G. B. Noe, C. R. Hupp, K. W. Krauss, N. B. Rybicki and E. R. Schenk, Soil greenhouse gas emissions and carbon budgeting in a short-hydroperiod floodplain wetland, *J. Geophysical Research: Biogeoscience*s, 2015, **120**, 77–95.

90 J. Audet, L. Elsgaard, C. Kjaergaard, S. E. Larsen and C. C. Hoffmann, Greenhouse gas emissions from a Danish riparian wetland before and after restoration, *Ecol. Eng.*, 2013, **57**, 170–182.
91 W. Merbach, T. Kalettka, C. Rudat, and J. Augustin, (2002). Trace gas emissions from riparian areas of small eutrophic inland waters in Northeast-Germany. In Wetlands in central Europe (pp. 235-244). Springer, Berlin, Heidelberg.
92 X. Wen, V. Unger, G. Jurasinski, F. Koebsch, F. Horn, G. Rehder, T. Sachs, D. Zak, G. Lischeid, K.H. Knorr, and M.E. Böttcher, Predominance of methanogens over methanotrophs in rewetted fens characterized by high methane emissions, *Biogeosciences*, 2018, **15**, 6519-6536.
93 S. A. F. Bonnett, M. S. A. Blackwell, R. Leah, V. Cook, M. O'Connor and E. Maltby, Temperature response of denitrification rate and greenhouse gas production in agricultural river marginal wetland soils, *Geobiology*, 2013, **11**, 252–267.
94 J. Gomez, P. Vidon, J. Gross, C. Beier, J. Caputo and M. Mitchell, Estimating greenhouse gas emissions at the soil–atmosphere interface in forested watersheds of the US Northeast, *Environ. Monitoring Assessment*, 2016, **188**, 295.
95 C.J. Talbot, J. Ceara, E.M. Bennett, K. Cassell, D.M. Hanes, E.C. Minor, H. Paerl, P.A. Raymond, R. Vargas, P.G. Vidon, W. Wollheim, and M.A. Xenopoulos, The impact of flooding on aquatic ecosystem services, *Biogeochemistry,* 2018*,* **141**, 439-461.
96 G. E. M. Van der Lee, H. O. Venterink and N. E. M. Asselman, Nutrient retention in floodplains of the Rhine distributaries in the Netherlands, *River Res. Appl.*, 2004, **20**, 315–325.
97 G. B. Noe and C. R. Hupp, Retention of riverine sediment and nutrient loads by coastal plain floodplains, *Ecosystems*, 2009, **12**, 728–746.
98 D. Zak, B. Kronvang, M.V. Carstensen, C.C. Hoffmann, A. Kjeldgaard, S.E. Larsen, J. Audet, S. Egemose, C.A. Jorgensen, P. Feuerbach and F. Gertz, Nitrogen and Phosphorus Removal from Agricultural Runoff in Integrated Buffer Zones, *Environ. Sci. Tech.*, 2018, **52**, 6508-6517.
99 K. K. Moorhead, D. W. Bell and R. N. Thorn, Floodplain hydrology after restoration of a Southern Appalachian mountain stream, *Wetlands*, 2008, **28**, 632–639.
100 T. Newcomer-Johnson, S. Kaushal, P. Mayer, R. Smith, and G. Sivirichi, Nutrient retention in restored streams and rivers: A global review and synthesis, *Water*, 2016, **8**, 116.

Tables

Table 1. Precipitation magnitude of each storm event (cm), and soil moisture (vol/vol ± standard deviation) at baseflow conditions (BF)* and 24 and 72 hours post-storm at the near-stream (NS) and upper riparian (UP) zone locations**.**

Storm				Soil Moisture (vol/vol ± SD)			
ID	**Precipitation (cm)**	**Intensity (mm hr^{-1})**	**Duration (hr)**	**NS 24 hr**	**NS 72 hr**	**UP 24 hr**	**UP 72 hr**
1	3.15	A: 1.23, M: 3.0	35	0.54±0.12	0.36±0.08	0.20±0.02	0.17±0.01
2	6.35	A: 0.61, M: 2.3	82	0.38±0.03	0.37±0.06	0.33±0.08	0.24±0.02
3	1.65	A: 2.3, M: 5.1	2	0.40±0.10	0.34±0.06	0.24±0.05	0.21±0.05

* BF Soil Moisture: NS (0.18±0.05); UP (0.14±0.04), A=average (mean), M=maximum

Table 2. Hydrologic parameters (hydraulic gradient, groundwater flux (liters/day), average water table height above an arbitrary datum [meters]) and nutrient (soluble reactive phosphorus [SRP] and nitrate [NO_3^-]) removal (percent) at baseflow (BF) conditions and 24 and 72 hours post-storm during the three storm events studied (see Table 1).

Storm ID	**Time Post-Storm (hrs)**	**Hydraulic Gradient**	**Groundwater Flux (L d^{-1})**	**Water Table Height (m)**	**NO_3^- Removal (%)**	**SRP Removal (%)**
BF	BF	0.022	7.36	1.36	92	78
1	24	0.031	10.53	1.53	93	26
1	72	0.024	8.2	1.36	96	79
2	24	0.020	6.6	1.48	95	83
2	72	0.019	6.4	1.37	92	89

3	24	0.013	4.44	1.22	89	51
3	72	0.016	5.52	1.22	92	9

Table 3. Significant Spearman's Rank variables of interest; Spearman's rho and p values are displayed for significant relationships between environmental parameters. Parameter abbreviations: SRP = soluble reactive phosphorus, WT = water table, N_2O = nitrous oxide, TDN = total dissolved nitrogen, NO_3^- = nitrate, CH_4 = methane, CO_2 = carbon dioxide.

Variable	**By Variable**	**Spearman's rho**	**p value**
SRP	WT height	0.28	0.177
SRP	N_2O	0.43	0.0002
SRP	TDN	0.51	<0.0001
SRP	NO_3^-	0.39	0.0010
TDN	N_2O	0.44	0.0002
NO_3^-	N_2O	0.47	<0.0001
NO_3^-	TDN	0.90	<0.0001

N_2O	CH_4	-0.24	0.0470
CO_2	Storm magnitude	-0.26	0.279

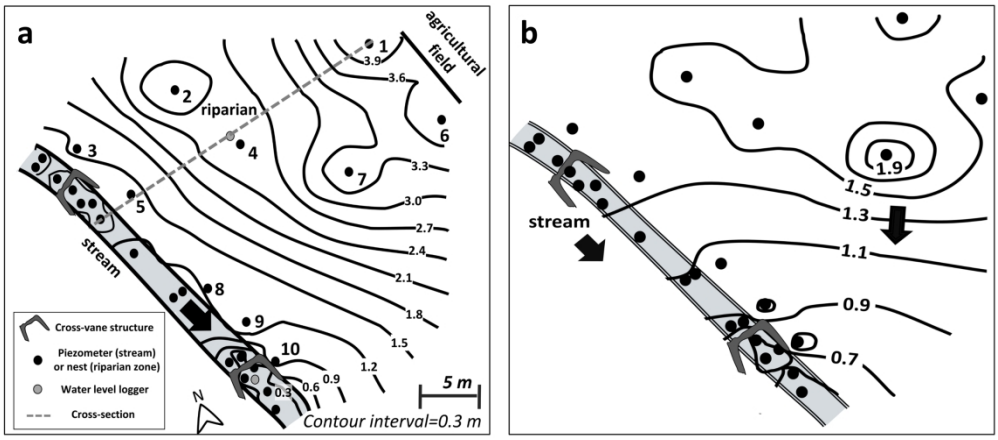

Figure 1. (a) Riparian topography, expressed in meters (m) above an arbitrary datum. Locations of individual in-stream piezometers and riparian nests (black circles) and water level loggers (gray circles) are displayed. Upper riparian (UR) piezometer nests are located on the hillslope and near-field (IDs: 1, 2, 4, 6, 7). Near-stream (NS) piezometer nests are located in the regraded section of the riparian zone (IDs: 3, 5, 8, 9, 10). Restoration structures (cross-vanes) are shown. The dashed line corresponds to a surveyed riparian stream cross-sectional profile. (b) Baseflow water table elevation contours in m above an arbitrary datum (lowest point on the streambed). Arrows show the direction of water flow.

247x108mm (300 x 300 DPI)

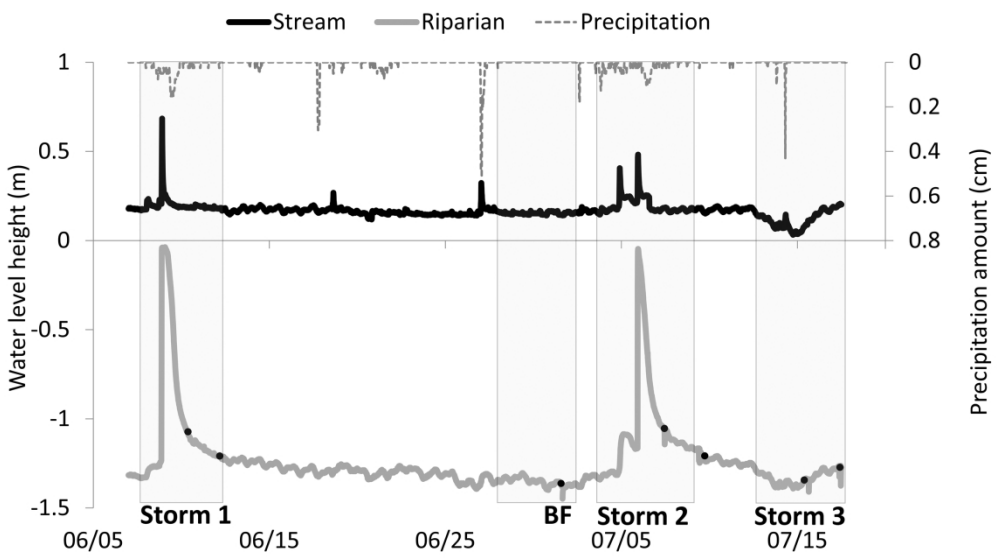

Figure 2. Hydrographs (primary y-axis, 15-min intervals) of stream stage (m above streambed, black line) and riparian zone water level (m below ground surface, denoted by negative water level values, gray line). Continuous 30 min precipitation in centimeters (cm) (dashed line, secondary y-axis) for the storm sampling period in June – July 2015 is also displayed. Storm 1 (3.15 cm), storm 2 (6.35 cm), and storm 3 (1.65 cm), as well as baseflow (BF) conditions, are denoted by gray boxes surrounding each storm event. Black dots on the riparian hydrograph indicate sampling times. Note: Precipitation hyetograph is based on a weather station 4.5 km away from the sites, so displayed absolute precipitation amounts are slightly different than amounts obtained from precipitation gages installed on-site.

224x125mm (300 x 300 DPI)

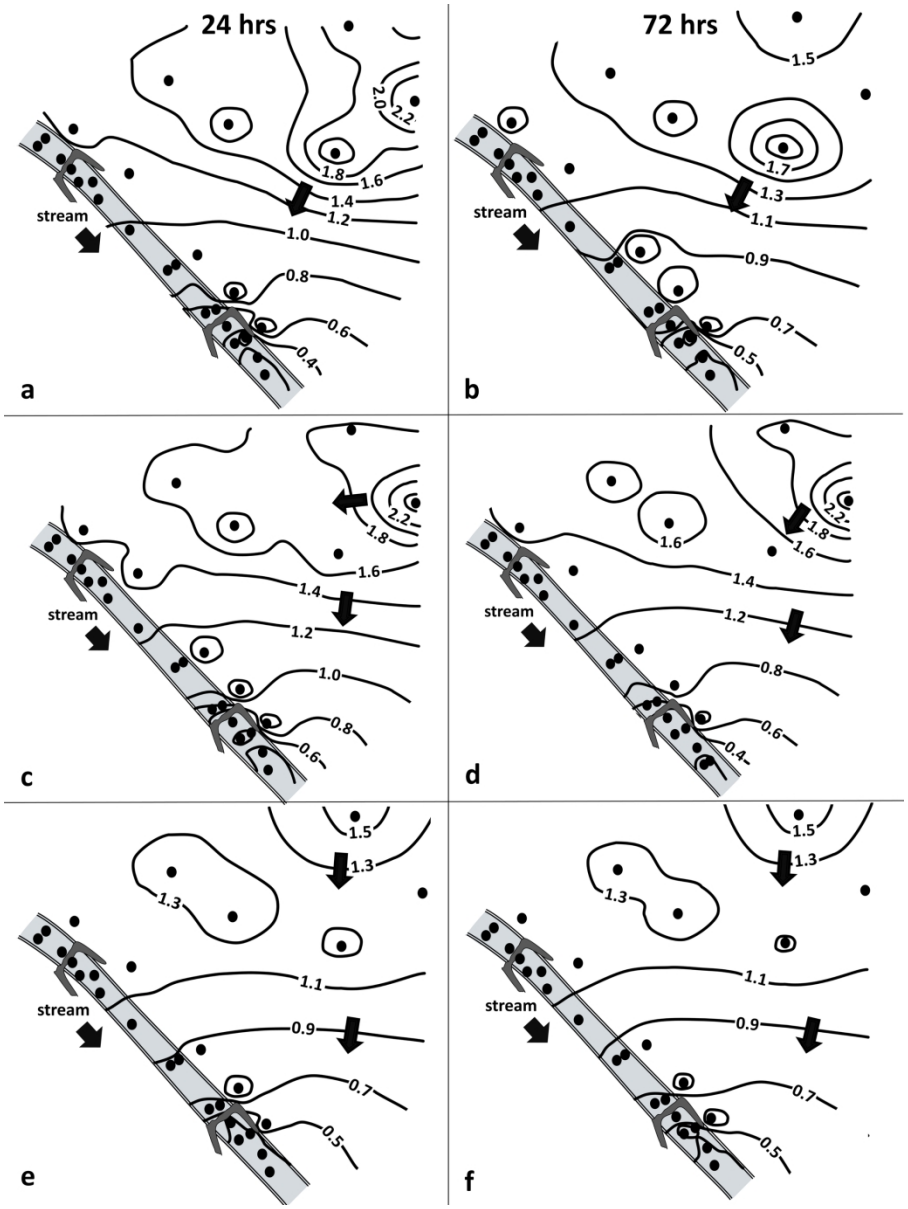

Figure 3. Riparian water table elevations, expressed in meters (m) above an arbitrary datum at 24 and 72 hours following three storms (Storm 1 [a, b], Storm 2 [c, d], and Storm 3 [e, f]). Arrows represent the general direction of groundwater flow. Groundwater mounding typically occurred at nest 7.

190x254mm (300 x 300 DPI)

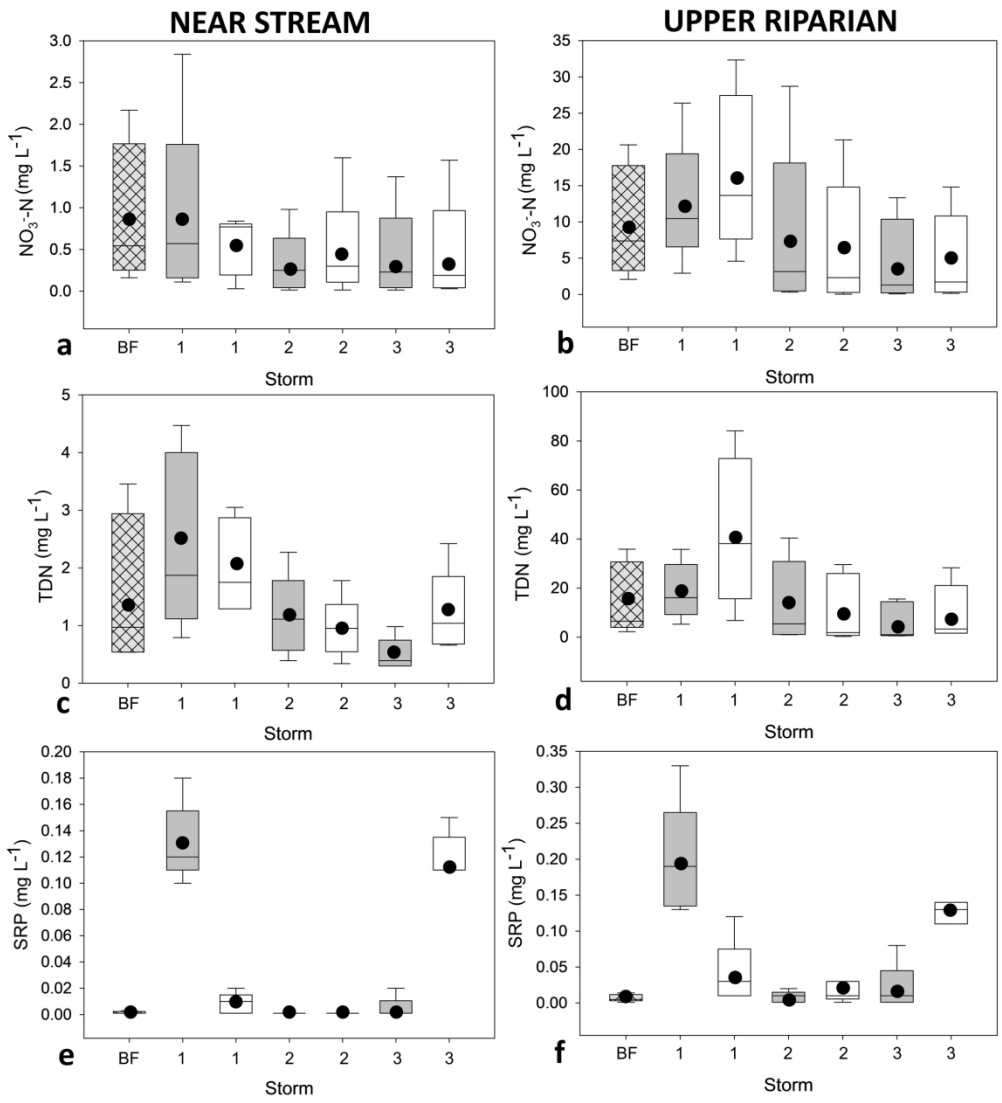

Figure 4. Boxplots (mean [black circle], median, 25th and 75th percentiles [box] and 5th/95th percentiles [whiskers]) of water chemistry in the upper (UP) and near stream (NS) riparian zone at 24 (gray box) and 72 (white box) hours post-storm for three storms for nitrate (NO_3^--N), soluble reactive phosphorus (as orthophosphate, PO_4^{3-}-P), and total dissolved nitrogen (TDN). BF = Baseflow conditions (hatched box).

188x207mm (300 x 300 DPI)

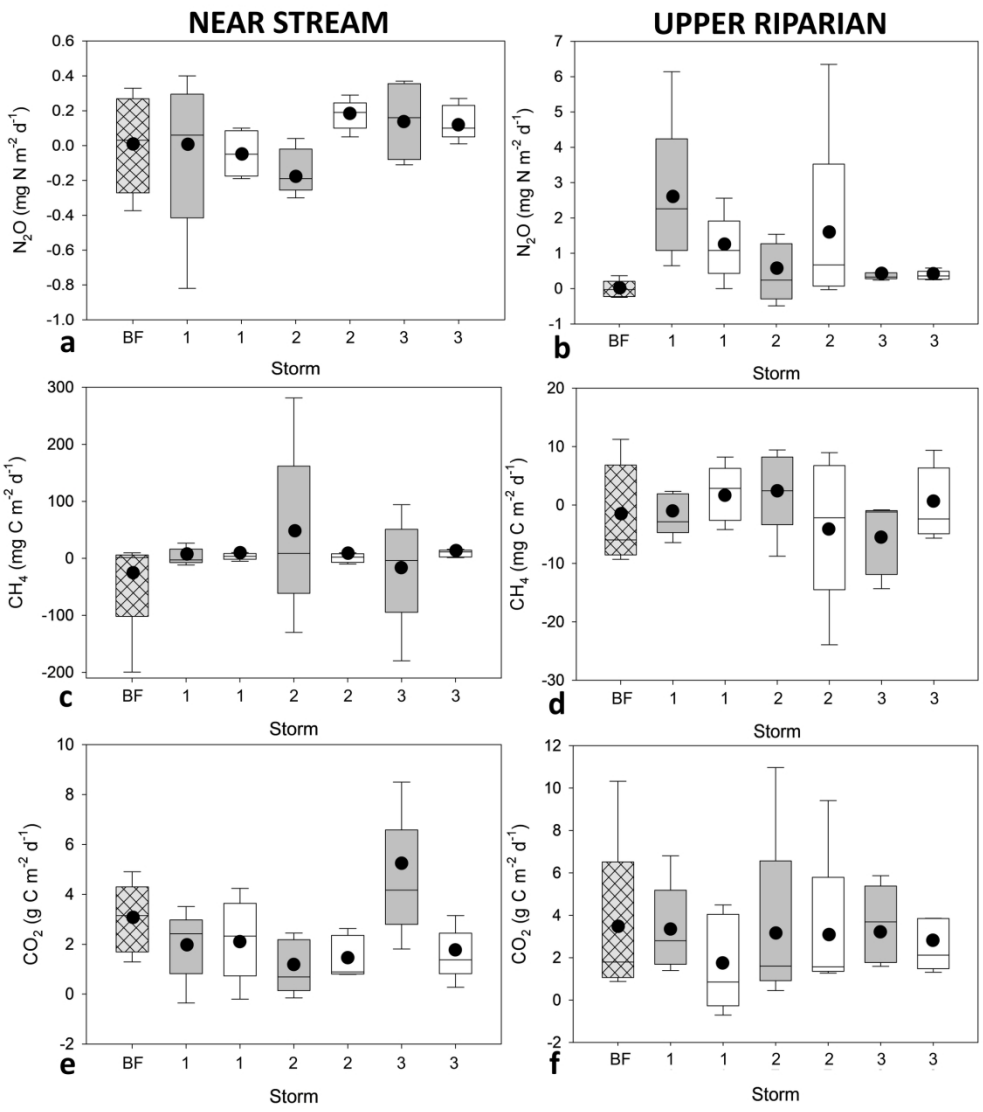

Figure 5. Boxplots (mean [black circle], median, 25th and 75th percentiles [box] and 5th/95th percentiles [whiskers]) showing fluxes of greenhouse gases (GHGs: carbon dioxide [CO_2], methane [CH_4], nitrous oxide [N_2O]) at the near stream (NS) and upper riparian (UP) zone locations at 24 (gray box) and 72 (white box) hours. Outliers were removed so the range of values within the 5 to 95 quartile could be seen. BF = Baseflow conditions (hatched box).

189x209mm (300 x 300 DPI)

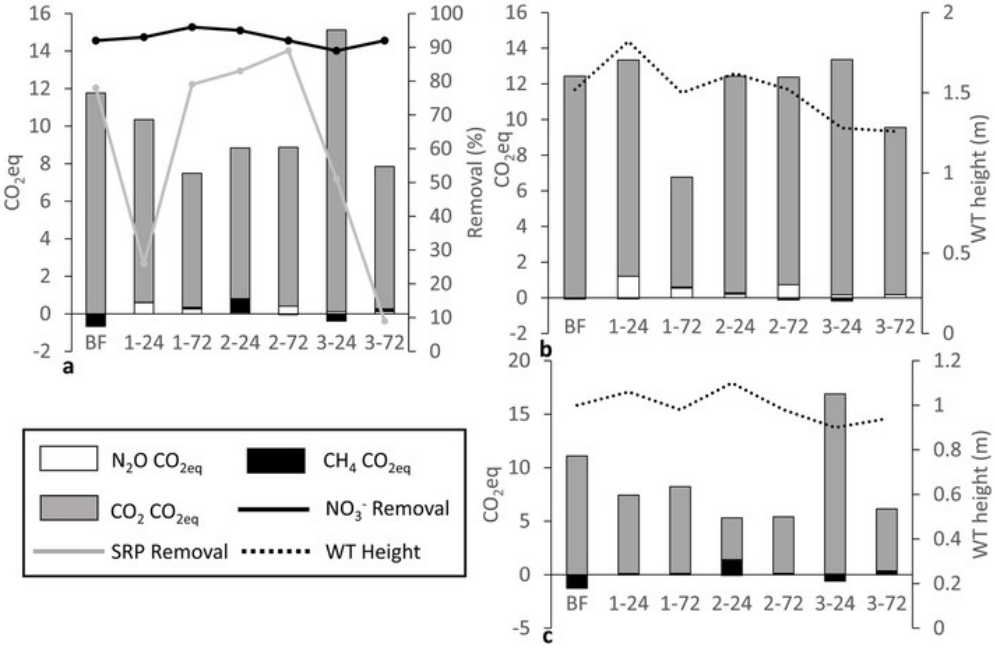

Figure 6. Average greenhouse gas (GHG: CO_2, N_2O, CH_4) emissions across the whole riparian zone (a), upper riparian zone (b), and near-stream zone (c), expressed as CO_2 equivalents (CO_{2eq}). Nitrate (NO_3^-) and soluble reactive phosphorus (SRP) removal across the riparian zone is displayed concurrently with GHG data (a), while average water table (WT) height is displayed alongside GHG fluxes by riparian location (upper and near-stream) (b, c).

189x124mm (96 x 96 DPI)

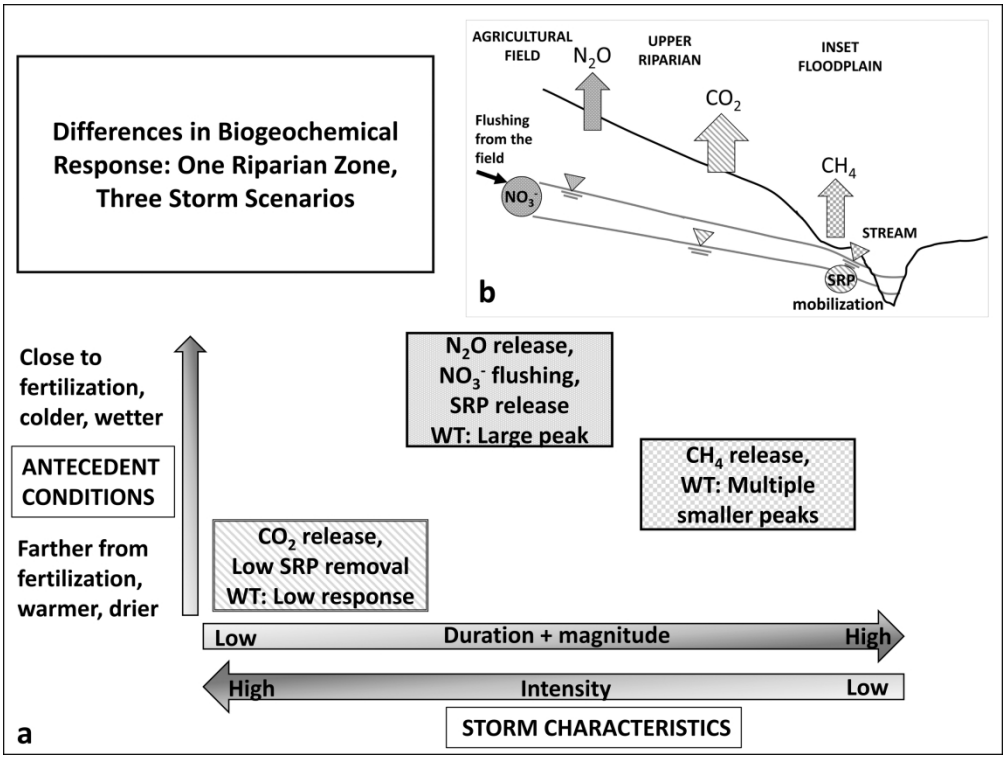

Figure 7. Conceptual model for three different storms, illustrating that storm types across a range of antecedent conditions, duration, magnitude, and intensity may have different biogeochemical responses. This diagram serves as a simplified illustration of the capacity for riparian zones to have different biogeochemical responses across a range of conditions (a) and indicates where potential "hot spots" of nutrient/gas mobilization and export may occur (b). The background pattern of each descriptive hydrologic/biogeochemical response box in diagram a corresponds to the pattern used in greenhouse gas flux arrows and nutrient circles in diagram b. Abbreviations: CO_2 = carbon dioxide, CH_4 = methane, N_2O = nitrous oxide, NO_3^- = nitrate, SRP = soluble reactive phosphorus, WT = water table.

254x190mm (300 x 300 DPI)

Table of Contents Entry

Storm timing, characteristics (duration, magnitude, and intensity), and antecedent conditions influence pollutant release and retention in riparian zones.